Electronic Supplementary Material (ESI) for Chemical Communications

Supporting Information

Mechanochromic Luminescent Property of A Polypeptide-based Dendron

Mingjun Teng , Xinru Jia* , Xiaofang Chen , Zhiyong Ma and Yen Wei

xrjia@pku.edu.cn

Experimentals

^{1}H NMR was recorded on 400 MHz (Bruker ARX400) and ^{13}C NMR spectra were recorded on Bruker 100 MHz spectrometer at room temperature with DMSO as the solvents and tetramethylsilane (TMS) as the internal standard. ESI high resolution mass-spectra (HRMS) were acquired on a Bruker Apex IV FTMS mass spectrometer. Differential scanning calorimetry (DSC) measurements were carried out on TA Instruments DSC Q100. Polarized optical microscopy (POM) images were recorded using a Leica DLMP microscope. 1D small angle X-ray scattering (SAXS) experiments were performed with a SAXS instrument (SAXSess, Anton Paar) equipped with Kratky block-collimation system. The scattering patterns of SAXS were simultaneously recorded on an imaging plate (IP) with a pixel size of $42.3\times42.3\mu m^2$ which extended to high-angle range (the q range covered by the IP was from 0.06 to 29 nm^{-1}). The scattering peak positions were calibrated with silicon powder for wide-angle region and silver behenate for small-angle region, respectively. After background subtraction, desmearing was performed according to the Lake's method. 1D WAXD powder experiments were performed on a Philips X'Pert Pro diffractometer with a 3 kW ceramic tube as the X-ray source (Cu KR) and an X'celerator detector. The reflection peak positions were calibrated with silicon powder ($2\theta > 15°$) and silver behenate ($2\theta < 10°$). FT-IR spectrum was obtained using a *Nicolet Magna IR-750 spectrometer* in a CaF_2 plate. UV-vis spectra were acquired on a Varian CARY 1E UV-vis spectrophotometer. Fluorescence spectra and the calculation of quantum yield were performed on the Nanolog/ FluoroLog-3-2- Ihr320

combined measurement system for infrared fluorescence equipped with an integrating sphere. Fluorescence decay spectra were measured on FLS 920 lifetime and steady state spectrometer (λ_{ex} = 345 nm). Geometry optimization of **1** was performed by "Forcite" modules in Material Studio Modeling 5.0 Software package. Atomic force microscopy (AFM) measurement was implemented on a SPA-400 multimode AFM and SPI3800N probe station.

1. Synthesis of 1

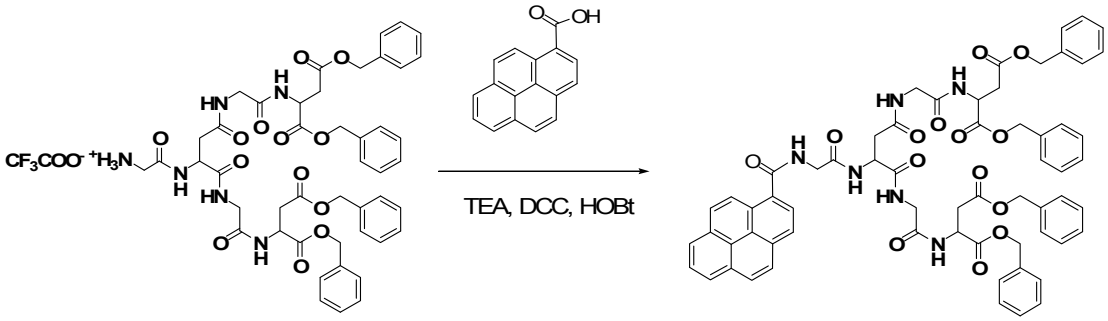

Gly-Asp G2-$NH_3^+CF_3COO^-$ (280 mg, 0.28 mmol) [1], TEA (0.5 mL) and 1-pyrenecarboxylic acid (82 mg 0.33 mmol) were mixed in chloroform (20 mL) with stirring in ice-salt bath. N,N'-dicyclohexylcarbodiimide (86 mg, 0.42 mmol) and N-Hydroxybenzotriazole (10 mg, 0.074 mmol) was added after 10 min. The reaction mixture was stirred for 2 day and concentrated under vacuum. Pure 1 (green solid) was obtained by the purification of silica gel column chromatography using $CHCl_2$/THF (5:1) as the eluent (yield 58%).

^{1}H NMR (400 MHz, DMSO, TMS, *T* = 298 K): 8.67-8.64 (d, 1H, pyrene-H), 8.51-8.10 (m, 8H, pyrene-H), 7.34-7.29 (m, 20H, Ph-H), 5.08-5.02 (m, 8H, -C*H*$_2$-Ph), 4.78-4.69 (m, 3H, -C*H*-), 4.16-4.05 (m, 2H,-C*H*$_2$-), 3.83-3.70 (m, 4H,-C*H*$_2$-), 2.94-2.60 (m, 6H, -C*H*$_2$-).

^{13}C NMR (400 MHz, DMSO, TMS, *T* = 298 K): 171.11, 170.29, 169.89, 169.81, 169.78, 169.70, 169.36, 169.28, 169.08, 168.89, 168.73, 135.77, 135.65, 131.69, 131.37, 130.69, 130.21, 128.36, 128.00, 127.96, 127.87, 127.65, 127.62, 127.18, 126.55, 125.76, 125.59, 125.32, 124.91, 124.35, 123.75, 123.63, 66.25, 65.86, 49.82, 48.50, 42.70,41.87, 37.38, 35.72.

Element Cal. For $C_{63}H_{58}N_6O_{14}$. C, 67.37; H, 5.20, N, 7.48. Found. C, 67.19; H, 5.47, N, 7.43. HR-ESI Cal. For $C_{63}H_{58}N_6O_{14}$: 1122.4011. Found. [M+H]: 1123.4071

2. Fluorescence decay profile of 1 in solution, drop cast aggregates and ground solids.

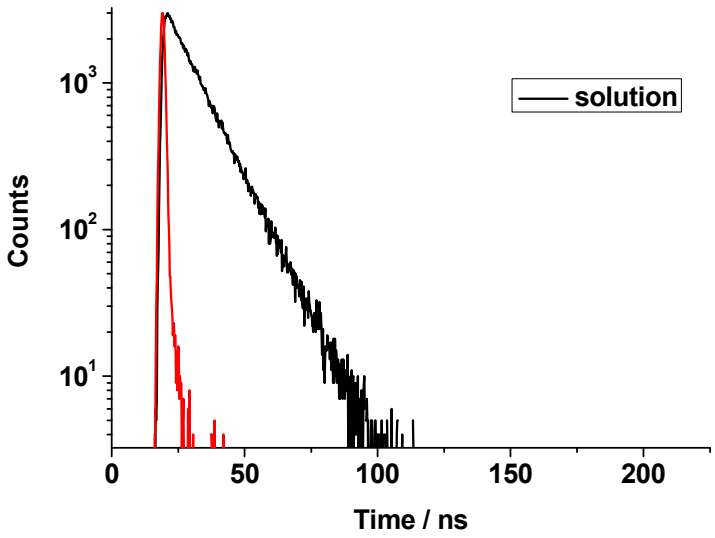

Figure S1. Fluorescence life time decay profile of **1** in CH_2Cl_2 solution (black) and instrument response function (red).

.

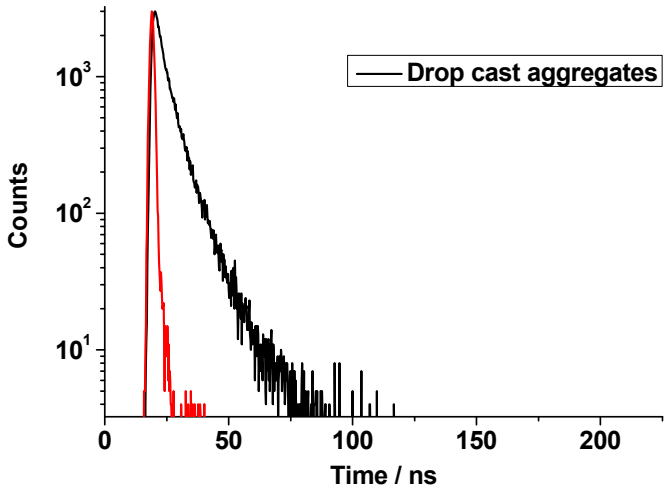

Figure S2. Fluorescence life time decay profile of drop cast aggregates (black) and instrument response function (red).

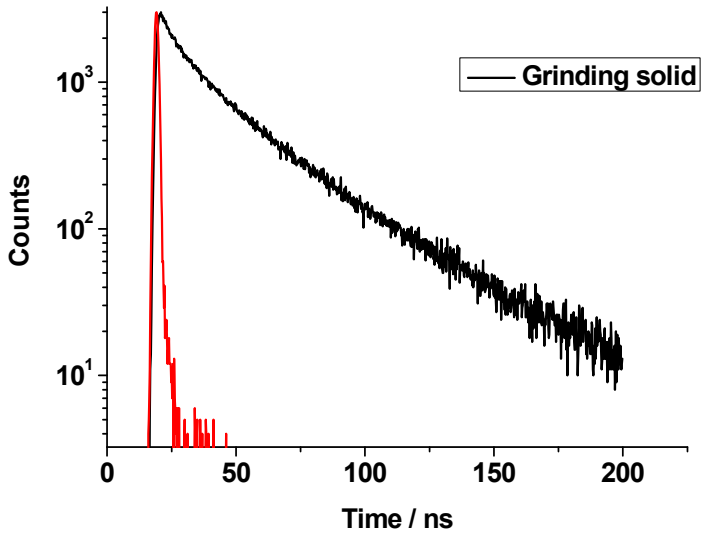

Figure S3. Fluorescence life time decay profile of grinding solid (black) and instrument response function (red).

.

3. UV-vis spectra of 1 in different states.

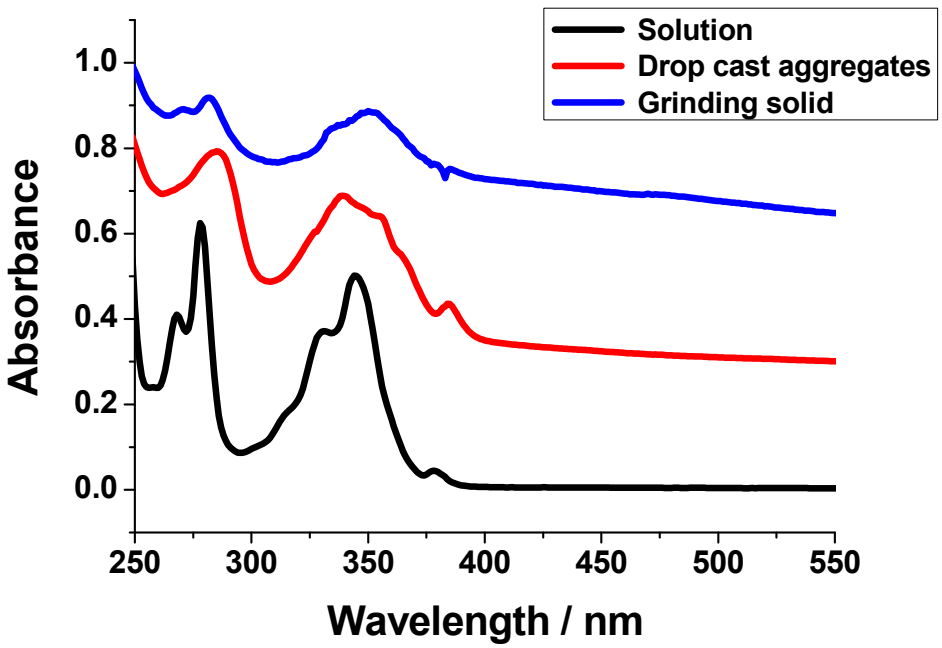

Figure S4. The absorption spectra of **1** in different states.

4. The optimized geometry of 1.

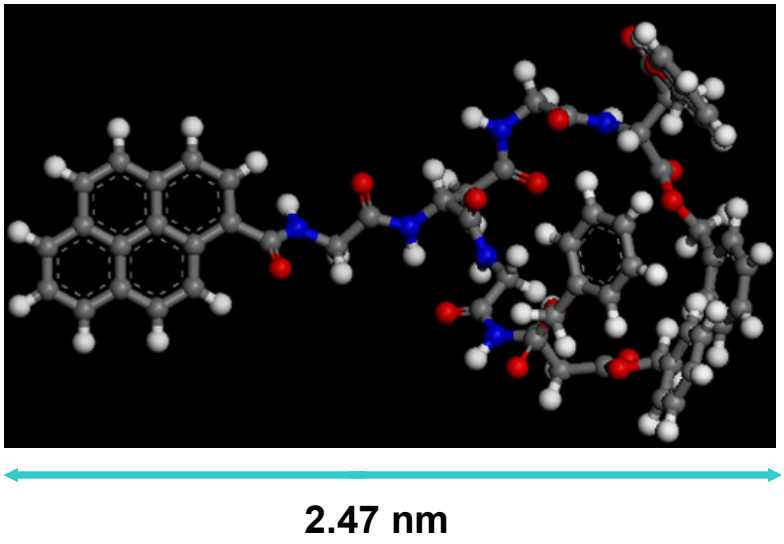

Figure S5. The optimized geometry of **1** in the gas phase calculated by using Forcite in Material Studio 5.0

5. Illustration of self-assembled structure of 1 in drop cast aggregates.

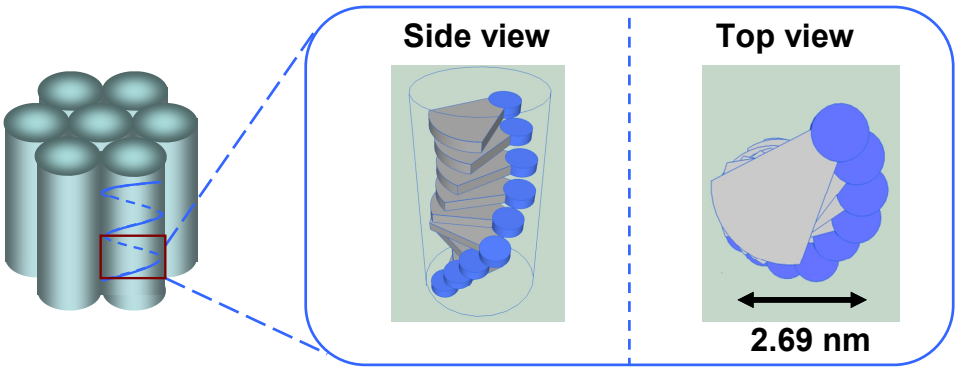

Figure S6. Illustration of self-assembled structure of **1** in drop cast aggregates.

6. Illustration of self-assembled structure of 1 in grinding solid.

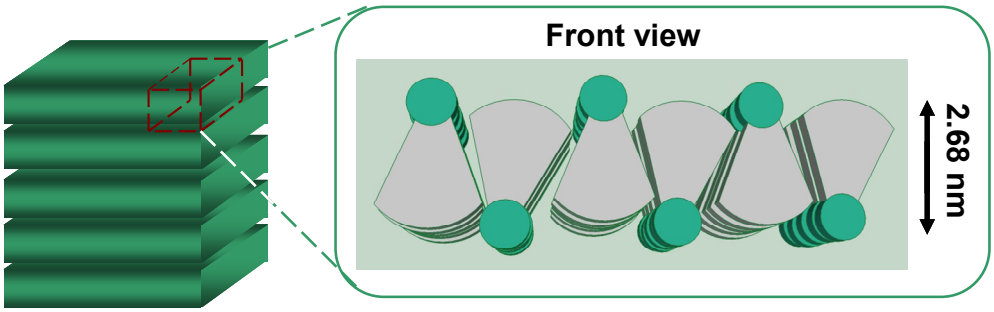

Figure S7. Illustration of self-assembled structure of **1** in grinding solid.

7. SAXS profiles of 1 in different states.

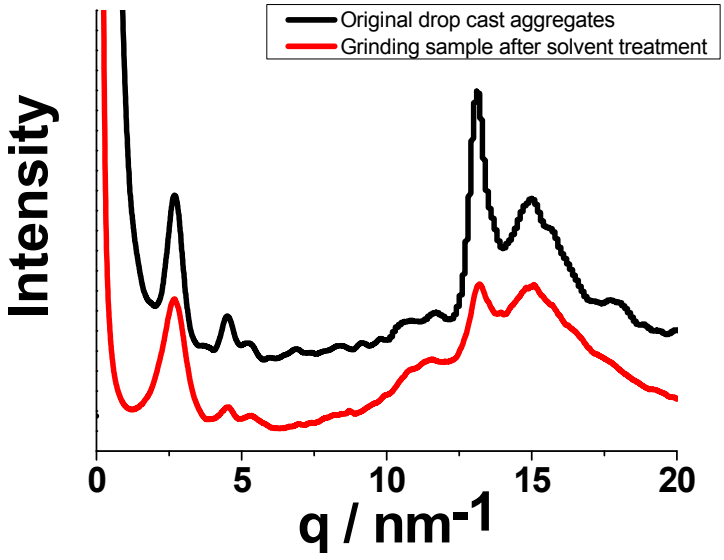

Figure S8. SAXS profiles of original drop cast aggregates (black lines) and grinding solid treated with CH_2Cl_2 (red line).

8. Infrared absorption of 1 in different states

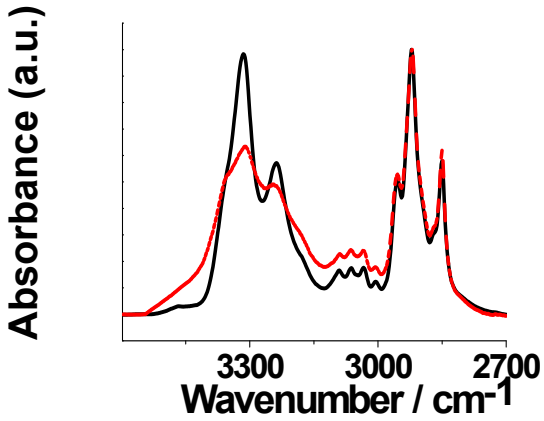

Figure S9. Infrared absorption of **1** before (black) and after grinding (red). (normalized to the C-H stretching at 2922 cm^{-1}).

9. Thermoanylasis profiles of 1.

The heating process was kept at the rate of 10 ^{o}C/min. The thermal gravimetric analysis (TGA) profile exhibited no decomposition of **1** during the temperature range.

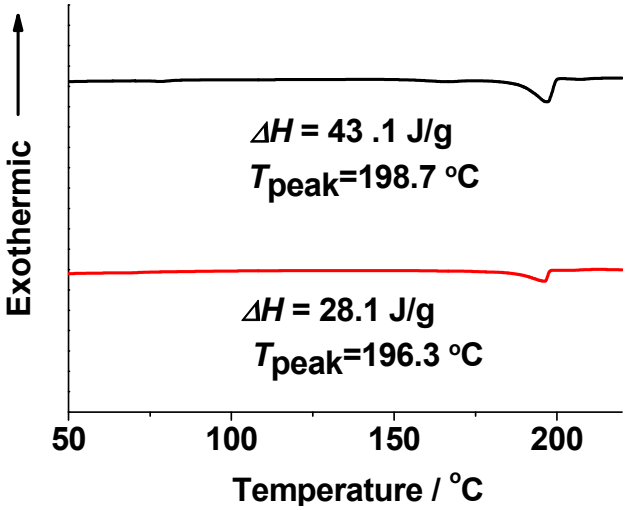

Figure S10. DSC profiles of drop cast aggregates (black) and finely grinding sample (red).

10. Fluorescent spectra of 1 at different cooling rates..

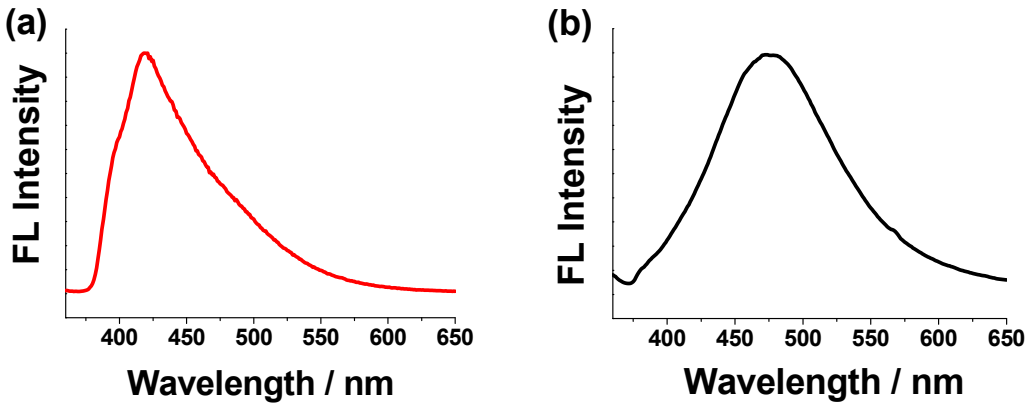

Figure S11. The fluorescence of **1** under different processing conditions. a) slow cooling at 10 ^{o}C/min from isotropic state. b) fast quenching from isotropic state.

11. Visual observation and AFM images of 1 at different cooling rates.

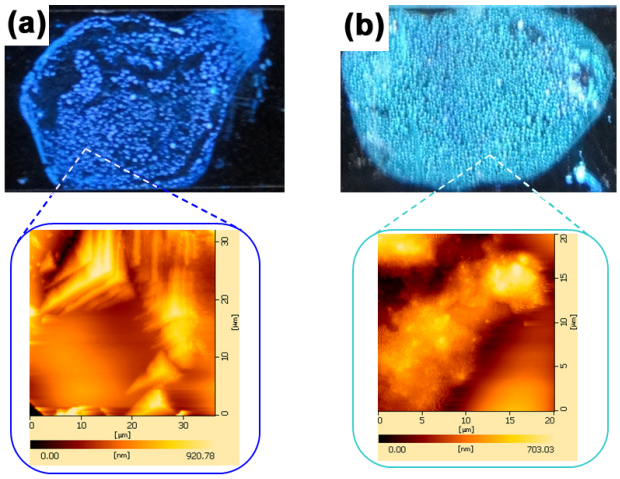

Figure S12. Visual observation under 365 nm UV light (up) and AFM images (down) of **1** at room temperature by a) cooling at less than 10 ^{o}C/min from isotropic state; b) fast quenching from isotropic state.

12. WAXD pattern for drop cast aggregates 1 at different cooling rates.

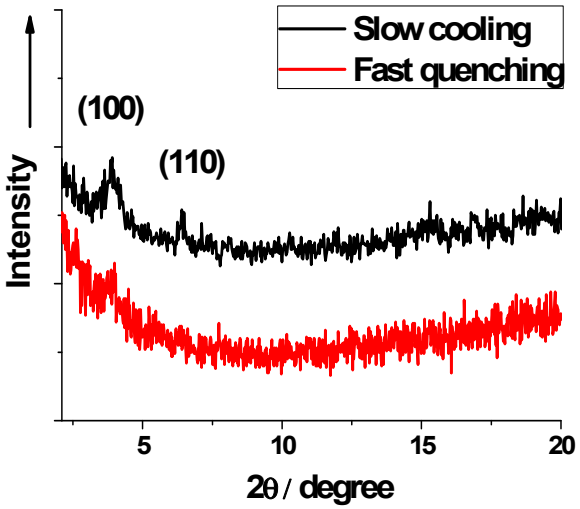

Figure S13. WAXD patterns for drop cast aggregates **1** at different cooling rates from isotropic state.

13. Photopatterned images prepared by drop cast aggregates of 1.

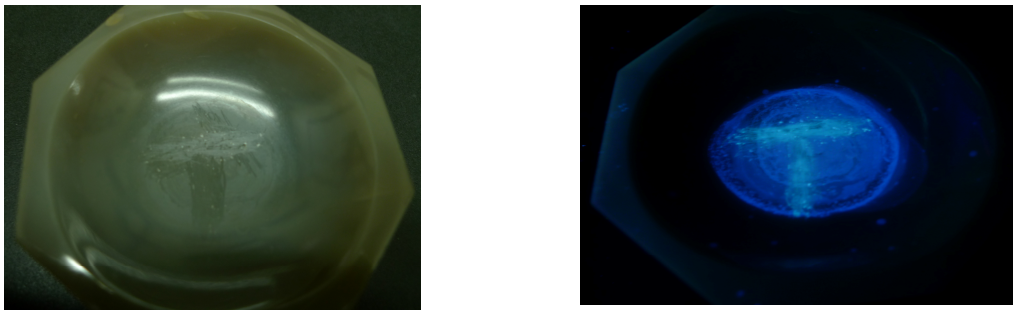

Figure S14. The drop cast aggregates of **1** with "T" shape shearing under ambient light (left) and 365 nm UV light irradiation (right).

Reference

[1] Y. Ji, Y. F. Luo, X. R. Jia, E. Q. Chen, Y. Huang, C. Ye, B. B. Wang, Q. F. Zhou and Y. Wei, *Angew. Chem. Int. Ed.* 2005, **44**, 6025.